HIGHAM FERRERS, Northamptonshire: Archaeomagnetic Dating Report 2002

Paul Linford

Summary

During archaeological excavations at a site containing Anglo-Saxon remains in Higham Ferrers, Northamptonshire, a well pottery kiln was uncovered, in association with pottery of the Late Medieval Reduced Ware tradition. Prior to this discovery, no well preserved kiln connected to the industry had been excavated, so the present example offers a unique opportunity to obtain a scientific date for an important regional pottery typology. So far the typology has been dated using documentary evidence, which refers to the purchase of land containing a kiln in Higham Ferrers and then its later refurbishment, during the latter half of 15th century AD.

Archaeomagnetic analysis of the structure demonstrated it to be well fired but with some magnetic distortion to the remanence directions of the samples taken from the kiln wall lining. However, an archaeomagnetic date of good precision was obtained for the last firing of the kiln, dating this event to the early part of the 15th century AD. The archaeomagnetic date suggests that the kiln analysed in this report is not the one referred to in the documents and that reduced ware production at Higham Ferrers might have begun earlier than previously supposed.

HIGHAM FERRERS, Northamptonshire:
Archaeomagnetic Dating Report 2002

Introduction

During archaeological excavations in Higham Ferrers town centre in advance of redevelopment work, a well preserved, late medieval pottery kiln was discovered, complete with substantial quantities of pottery wasters (Latitude 52.3°N, Longitude 0.6°W, OSNGR: SP 959 692). Examination of the pottery indicated that the kiln had been involved in the production of Late Medieval Reduced Ware, a broad pottery tradition common throughout the East Midlands between about 1350 and 1550 AD. Prior to this discovery, no well preserved kiln associated with this industry has been found, hence this example offers a unique opportunity to obtain a scientific date for an important regional pottery typology. Documentary evidence refers to the purchase of land containing a kiln in Higham Ferrers, and its later refurbishment, during the latter half of 15th century AD (Paul Blinkhorn *pers. comm.*). However, the location of the site described has not been identified and it is possible that these remains relate to it.

Figure 1; Photograph of the Higham Ferrers kiln during archaeomagnetic sampling, viewed from the west. The quadrant containing samples 01-11(see Figure 2) is visible in the centre of the picture.

Most of the archaeological features uncovered by the excavation date from the Anglo-Saxon period and their evaluation was supported by funding through the PPG16 process. However, it was felt that a proper investigation of the medieval kiln went beyond the remit of the developer funded project and English Heritage (EH) was asked to assist. Hence, with the support of the EH Inspector of Archaeological Monuments for the region, Glyn Copack, the Centre for Archaeology (C*f*A) provided archaeomagnetic analysis of the feature. It was sampled on the 14th of May 2002 by the author who also carried out the subsequent measurement and evaluation. Figure 1 shows a photograph of the kiln remains during the sampling exercise.

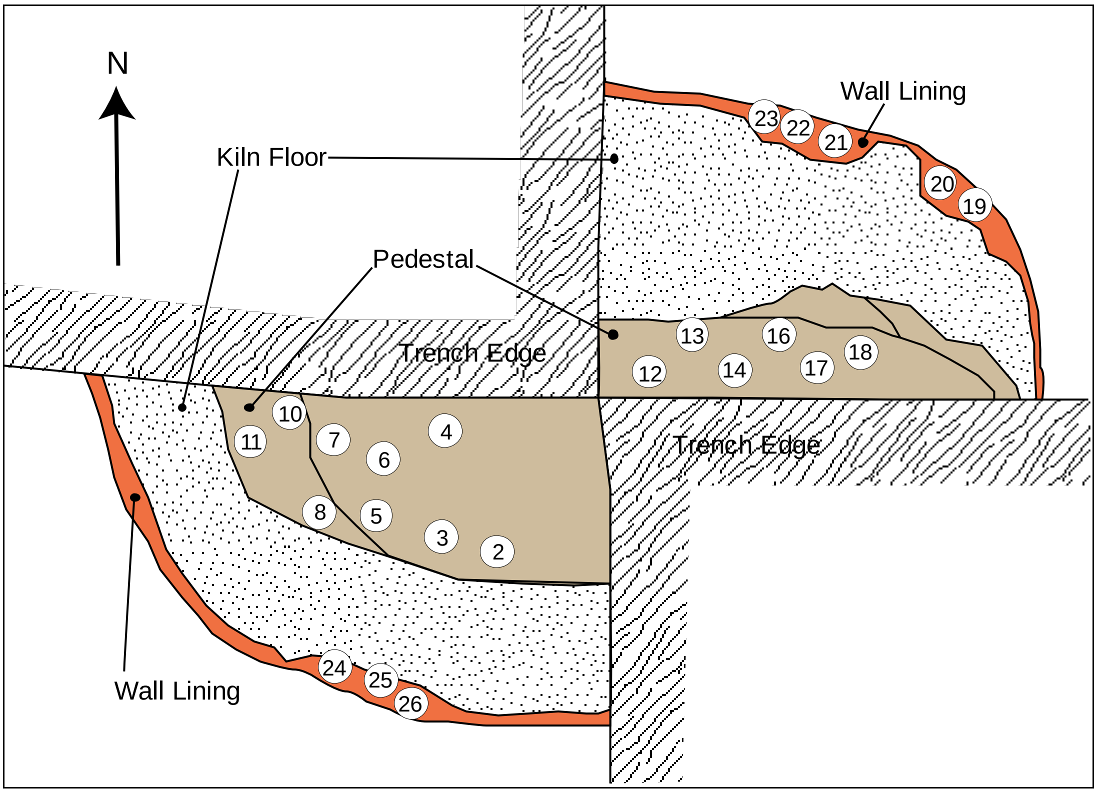

Figure 2; Sketch plan of the Higham Ferrers kiln showing the locations of the archaeomagnetic samples.

Method

The feature was given the C*f*A archaeomagnetic feature code HF. Samples were collected from it using the disc method (see appendix, section 1a) and orientated to magnetic north using a compass. Subsequently the International Geomagnetic Reference Field (IGRF 2000) was used to establish that magnetic north was 3.2° west of true north at the site on the date when the samples were taken and the sample orientations were corrected accordingly. Twenty-three samples were collected from the pedestal and wall lining of the kiln as indicated in the sketch plan shown in Figure 2 (Samples 01 and 09 fragmented on extraction, the number 15 was not used as a sample identifier). All but two of the samples were of very well fired clay: those from the pedestal (samples numbers <= 18) were yellow/grey in colouration; those from the wall lining (sample numbers > 20) were a more orange colour. The two exceptions, 19 and 20, were discovered on cleaning in the laboratory, to be of a whitish stone that had been incorporated into the wall lining.

The natural remanent magnetisation (NRM) measured in archaeomagnetic samples is assumed to be caused by thermoremanent magnetisation (TRM) created at the time when the feature of which they were part was last fired. However, a secondary component acquired in later geomagnetic fields can also be present, caused by diagenesis or partial reheating. Additionally, the primary TRM may be overprinted by a viscous component, depending on the grain size distribution within the magnetic material. These secondary components are usually of lower stability than the primary TRM and can thus be removed by partial demagnetisation of the samples.

A typical strategy used in archaeomagnetic analysis of a feature is first to measure the NRM field recorded in all the samples. Then a number of representative samples are selected for pilot partial demagnetisation depending upon their material composition and NRM characteristics. Partial demagnetisation involves exposing the sample to an alternating magnetic field of fixed peak strength then measuring the resulting changes in its magnetisation. This procedure is repeated with increasing peak field strengths to build up a complete picture of the coercivity spectrum of the sample. The equipment used for these measurements is described in section 2 of the appendix.

After inspection of the coercivity spectra of the pilot samples, an optimum field strength is selected where it is judged that the maximum amount of secondary magnetisation has been removed, whilst preserving the majority of the primary magnetisation. The remaining samples are then partially demagnetised using this optimum peak alternating field strength. In some cases the set of samples can be partitioned into groups with different material composition or magnetic characteristics. When this occurs several different field strengths may be used, each one judged to be the optimum for a particular group.

A mean TRM direction is calculated from the sample measurements made after partial demagnetisation at their optimum field strength. Some samples may be excluded from this calculation if their TRM directions are so anomalous as to make them statistical outliers from the overall TRM distribution. A “magnetic refraction” correction is often applied to the sample mean TRM direction to compensate for distortion of the earth’s magnetic field due to the geometry of the magnetic fabric of the feature itself. Then the mean is adjusted according to the location of the feature relative to a notional central point in the UK (Meriden), so that it can be compared with UK archaeomagnetic calibration data to produce a date of last firing for the feature. Notes concerning the mean calculation and subsequent calibration can be found in sections 3 and 4 of the appendix.

This measurement and calibration strategy was applied to the analysis of the samples from Higham Ferrers. All the samples used to calculate the mean TRM direction were taken from the pedestal, a horizontal surface, so a magnetic refraction correction of 2.4^{o} was added to this mean’s inclination before calibration.

Results

Sample NRM measurements and measurements after partial demagnetisation are recorded in Table 1. Figure 3 depicts the distribution of the sample TRM directions before and after partial demagnetisation. Table 2 records the pilot demagnetisation measurements made on samples 03, 14 and 25 whilst Figures 4-6 illustrate these results graphically.

The maximum stability of the TRM in each pilot sample was estimated using the method of Tarling and Symons (1967). The maximum stability parameters and ranges over which they persist are listed for each sample in Table 3. In this method, any sample with a maximum stability parameter greater than 2 is judged to record a stable TRM direction and a parameter value over 5 suggests extreme stability. The figures in Table 3 indicate that the magnetisations of all the pilot demagnetisation samples are extremely stable.

However, it can be seen from Table 1 that the stone samples, 19 and 20, have extremely low magnetisation intensities and highly anomalous directions. These results indicate that the stone did not contain a suitable magnetic mineralogy to acquire a stable remanent magnetisation. These two samples were thus excluded from further analysis.

It is also clear from Figure 1 that the other samples that came from the kiln wall lining (sample numbers > 20) all have steeper inclinations than those taken from the pedestal, which cluster to form the main grouping. Furthermore, inspection of the pilot demagnetisation results from sample 25 (see Figure 6), suggests that this effect is not due to perturbation by low stability viscous remanence. Such anomalous steepening of the inclinations of samples taken from strongly magnetised features has been noted previously. Samples taken from the walls of kilns have been found to have inclinations often several degrees steeper than those of samples taken from the floors of the same kilns. The phenomenon is not well understood but it has been suggested that it is due either to magnetic refraction caused by the shape of the structure (Aitken and Hawley, 1971; Schurr et al. 1984), or to the magnetisation of those parts of the feature that cool first distorting the magnetic field through the feature (Tarling et al., 1986). Owing to this uncertainty, the remaining kiln wall lining samples were omitted from the present analysis, directed towards dating the Higham Ferrers kiln, but have been retained for possible future research into the phenomenon of magnetic distortion.

Inspection of the most stable ranges of the pilot samples in Table 3 suggested that the optimum field strength for partial demagnetisation of the remaining samples (all from the kiln pedestal) was 5mT. The results of measurements made after applying this demagnetising field are tabulated in Table 1 and depicted in Figure 3b.

The mean TRM vector for the feature was calculated from the measurements made on the 15 pedestal samples after this 5mT partial demagnetisation:

At site: **Dec = 2.3 ^{o}** **Inc = 56.5 ^{o}** **α_{95} = 2.0^{o}** **k = 372.8**
At Meriden: **Dec = 2.0 ^{o}** **Inc = 56.6 ^{o}**

Figure 7 shows the comparison of the mean TRM vector with the UK archaeomagnetic calibration curve depicted on a Bauer plot. The date of the last firing of the kiln deduced from it is:

1395 AD to 1425 AD at the 63% confidence level.

1385 AD to 1435 AD at the 95% confidence level.

Conclusions

Archaeomagnetic analysis of the Higham Ferrers kiln has shown it to be well fired but with some magnetic distortion to the remanence directions of the samples taken from the wall lining. However, after rejecting these samples, it was still possible to obtain a mean TRM vector of good precision using the 15 samples taken from the central pedestal of the structure. From this mean TRM it was possible to deduce an archaeomagnetic date for the last firing of the kiln, indicating that this event occurred in the early part of the 15th century AD. This date suggests that the kiln analysed in this report is not the one referred to in the documentary evidence and that Late Medieval Reduced Ware production at Higham Ferrers might thus have begun earlier than previously supposed.

P. Linford
Archaeometry Branch,
Centre for Archaeology, English Heritage.

Date of report: 28/06/2002

Archaeomagnetic Date Summary

Archaeomagnetic ID:	**HF**
Feature:	**Late medieval clay lined pottery kiln**
Location:	**Longitude 0.6°W, Latitude 52.3°N**
Number of Samples (taken/used in mean):	**23/15**
AF Demagnetisation Applied:	**5mT**
Distortion Correction Applied:	**+2.4°**
Declination (at Meriden):	**2.3° (2.0°)**
Inclination (at Meriden):	**56.5° (56.6°)**
Alpha-95:	**2.0°**
k:	**372.8**
Date range (63% confidence):	**1395 to 1425 AD**
Date range (95% confidence):	**1385 to 1435 AD**
Independent date estimate:	**1350 AD to 1550 AD (for pottery typology)**

Sample	NRM Measurements				After Partial Demagnetisation				
	Material	Dec°	Inc°	J(mAm⁻¹)	AF(mT)	Dec°	Inc°	J(mAm⁻¹)	R
HF02	Clay	4.5	56.1	1712.5	5.0	3.5	54.9	1598.6	
HF03	Clay	1.4	47.0	2748.1	5.0	1.2	46.9	2495.3	
HF04	Clay	6.3	54.2	3297.0	5.0	7.1	53.0	3041.6	
HF05	Clay	2.2	52.4	2375.4	5.0	0.8	53.7	2209.8	
HF06	Clay	1.9	53.2	2524.5	5.0	0.1	52.7	2393.9	
HF07	Clay	-2.3	57.7	200.5	5.0	-2.1	57.0	176.9	
HF08	Clay	4.8	55.9	4078.4	5.0	5.9	57.6	3820.0	
HF10	Clay	-3.4	54.2	942.4	5.0	-4.6	53.5	886.3	
HF11	Clay	2.9	53.0	1428.4	5.0	1.2	53.6	1285.9	
HF12	Clay	-5.1	50.6	29.7	5.0	-0.6	48.2	26.4	
HF13	Clay	-2.7	55.4	1731.0	5.0	-4.2	54.9	1659.5	
HF14	Clay	13.3	57.3	2835.1	5.0	13.7	56.9	2672.4	
HF16	Clay	7.1	58.7	2036.6	5.0	6.5	57.9	1927.7	
HF17	Clay	-0.1	56.4	468.5	5.0	-0.7	56.1	442.2	
HF18	Clay	8.3	54.6	2945.8	5.0	8.7	53.0	2943.6	
HF19	Stone	63.2	-20.5	5.1	-	-	-	-	R
HF20	Stone	-136.6	46.1	5.0	-	-	-	-	R
HF21	Clay	-8.4	61.2	3896.5	-	-	-	-	R
HF22	Clay	-0.5	60.7	2182.4	-	-	-	-	R
HF23	Clay	-14.9	63.7	54.6	-	-	-	-	R
HF24	Clay	-13.7	74.8	4753.3	-	-	-	-	R
HF25	Clay	-6.5	69.1	3522.5	-	-	-	-	R
HF26	Clay	-8.3	73.8	2714.9	-	-	-	-	R

Table 1: NRM measurements of samples and measurements after partial AF demagnetisation for feature HF. J = magnitude of magnetisation vector; AF = peak alternating field strength of demagnetising field; R = sample rejected from mean calculation.

AF(mT)	HF03			HF14			HF25		
	Dec°	Inc°	J(mAm⁻¹)	Dec°	Inc°	J(mAm⁻¹)	Dec°	Inc°	J(mAm⁻¹)
0.0	0.6	47.8	2693.3	13.7	57.6	2830.3	-6.9	67.2	3535.1
1.0	1.0	47.8	2667.0	13.7	57.2	2811.7	-6.7	66.5	3522.6
2.5	1.2	47.7	2619.5	14.0	56.9	2771.8	-6.6	66.4	3486.1
5.0	1.2	46.9	2495.3	13.7	56.9	2672.4	-6.7	66.3	3404.5
10.0	0.7	46.1	2147.6	14.1	56.7	2268.3	-6.5	66.4	3060.8
15.0	-	-	-	13.9	56.2	1801.6	-6.0	66.8	2616.9
20.0	0.3	43.6	1459.8	13.6	55.6	1351.3	-5.1	66.5	2092.6
30.0	-0.4	42.1	985.3	13.8	54.9	760.3	-6.2	66.2	1495.5
50.0	-0.1	39.7	470.6	14.9	54.4	320.2	-4.9	65.9	965.1
75.0	0.0	35.6	199.8	16.5	47.3	168.3	-5.4	64.9	727.7

Table 2: Incremental partial demagnetisation measurements for samples HF03, HF14 and HF25.

Sample	Range min. (mT)	Range max. (mT)	Max. Stability	Dec°	Inc°
HF03	0.0	2.5	23.4	0.9	47.8
HF14	2.5	10.0	53.4	13.9	56.8
HF25	2.5	10.0	123.2	-6.6	66.4

Table 3: Assessment of the range of demagnetisation values over which each sample attained its maximum directional stability for feature HF, using the method of Tarling and Symons (1967). The declination and inclination values quoted are for the mean TRM direction for the sample calculated for all demagnetisation measurements in its range of maximum stability.

Appendix: Standard Procedures for Sampling and Measurement

1) Sampling

One of three sampling techniques is employed depending on the consistency of the material (Clark, Tarling and Noel 1988):

a) **Consolidated materials:** Rock and fired clay samples are collected by the disc method. Several small levelled plastic discs are glued to the feature, marked with an orientation line related to True North, then removed with a small piece of the material attached.

b) **Unconsolidated materials:** Sediments are collected by the tube method. Small pillars of the material are carved out from a prepared platform, then encapsulated in levelled plastic tubes using plaster of Paris. The orientation line is then marked on top of the plaster.

c) **Plastic materials:** Waterlogged clays and muds are sampled in a similar manner to method 1b) above; however, the levelled plastic tubes are pressed directly into the material to be sampled.

2) Physical Analysis

a) Magnetic remanences are measured using a slow speed spinner fluxgate magnetometer (Molyneux et al. 1972; see also Tarling 1983, p84; Thompson and Oldfield 1986, p52).

b) Partial demagnetisation is achieved using the alternating magnetic field method (As 1967; Creer 1959; see also Tarling 1983, p91; Thompson and Oldfield 1986, p59), to remove viscous magnetic components if necessary. Demagnetising fields are measured in milli-Tesla (mT), figures quoted being for the peak value of the field.

3) Remanent Field Direction

a) The remanent field direction of a sample is expressed as two angles, declination (Dec) and inclination (Inc), both quoted in degrees. Declination represents the bearing of the field relative to true north, angles to the east being positive; inclination represents the angle of dip of this field.

b) Aitken and Hawley (1971) have shown that the angle of inclination in measured samples is likely to be distorted owing to magnetic refraction. The phenomenon is not well understood but is known to depend on the position the samples occupied within the structure. The corrections recommended by Aitken and Hawley are applied, where appropriate, to measured inclinations, in keeping with the practise of Clark, Tarling and Noel (1988).

c) Individual remanent field directions are combined to produce the mean remanent field direction using the statistical method developed by R. A. Fisher (1953). The quantity $\boldsymbol{\alpha_{95}}$, "alpha-95", is quoted with mean field directions and is a measure of the precision of the determination (see Aitken 1990, p247). It is analogous to the standard error statistic for scalar quantities; hence the smaller its value, the better the precision of the date.

d) For the purposes of comparison with standardised UK calibration data, remanent field directions are adjusted to the values they would have had if the feature had been located at Meriden, a standard reference point. The adjustment is done using the method suggested by Noel (Tarling 1983, p116).

4) Calibration

a) Material less than 3000 years old is dated using the archaeomagnetic calibration curve compiled by Clark, Tarling and Noel (1988).

b) Older material is dated using the lake sediment data compiled by Turner and Thompson (1982).

c) Dates are normally given at the 63% and 95% confidence levels. However, the quality of the measurement and the estimated reliability of the calibration curve for the period in question are not taken into account, so this figure is only approximate. Owing to crossovers and contiguities in the curve, alternative dates are sometimes given. It may be possible to select the correct alternative using independent dating evidence.

d) As the thermoremanent effect is reset at each heating, all dates for fired material refer to the final heating.

e) Dates are prefixed by "cal", for consistency with the new convention for calibrated radiocarbon dates (Mook 1986).

References

Aitken, M. J. 1990. *Science-based Dating in Archaeology*. London: Longman.

Aitken, M. J. and H. N. Hawley 1971. Archaeomagnetism: evidence for magnetic refraction in kiln structures. *Archaeometry* **13**, 83-85.

As, J. A. 1967. The a.c. demagnetisation technique, in *Methods in Palaeomagnetism*, D. W. Collinson, K. M. Creer and S. K. Runcorn (eds). Amsterdam: Elsevier.

Clark, A. J., D. H. Tarling and M. Noel 1988. Developments in Archaeomagnetic Dating in Britain. *J. Arch. Sci.* **15**, 645-667.

Creer, K. M. 1959. A.C. demagnetisation of unstable Triassic Keuper Marls from S. W. England. *Geophys. J. R. Astr. Soc.* **2**, 261-275.

Fisher, R. A. 1953. Dispersion on a sphere. *Proc. R. Soc. London A* **217**, 295-305.

IGRF, 2000. International Geomagnetic Reference Field - Epoch 2000. Revision Of The IGRF for 2000 – 2005. *http://www.ngdc.noaa.gov/IAGA/wg8/igrf2000.html*

Molyneux, L., R. Thompson, F. Oldfield and M. E. McCallan 1972. Rapid measurement of the remanent magnetisation of long cores of sediment. *Nature* **237**, 42-43.

Mook, W. G. 1986. Recommendations/Resolutions Adopted by the Twelfth International Radiocarbon Conference. *Radiocarbon* **28**, M. Stuiver and S. Kra (eds), 799.

Schurr, K., Becker, H. and Soffel, H. C. 1984. Archaeomagnetic study of medieval fireplaces and ovens and the problem of magnetic refraction. *J. Geophys*. **56**, 1-8.

Tarling, D. H. 1983. *Palaeomagnetism*. London: Chapman and Hall.

Tarling, D. H., Hammo, N. B. and Downey, W. S. 1986. The scatter of magnetic directions in archaeomagnetic studies. *Geophysics* **51**, 634-639.

Tarling, D. H. and Symons, D. T. A. 1967. A stability index of remanence in palaeomagnetism. *Geophys. J. R. astr. Soc*. **12**, 443-448.

Thompson, R. and F. Oldfield 1986. *Environmental Magnetism*. London: Allen and Unwin.

Turner, G. M. and R. Thompson 1982. Detransformation of the British geomagnetic secular variation record for Holocene times. *Geophys. J. R. Astr. Soc.* **70**, 789-792.

a)

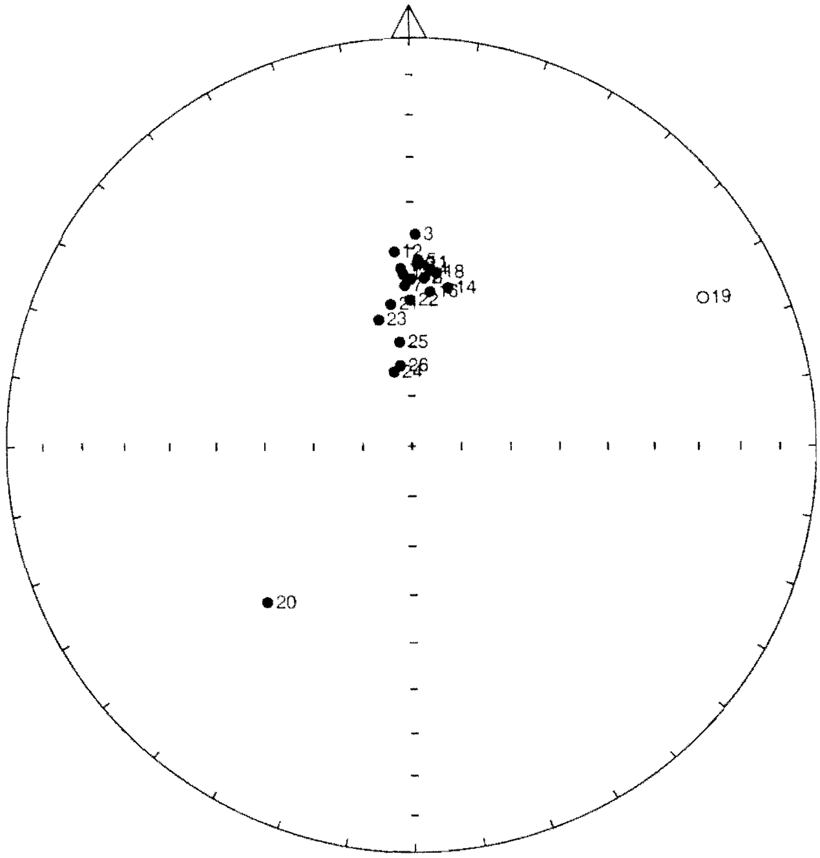

b)

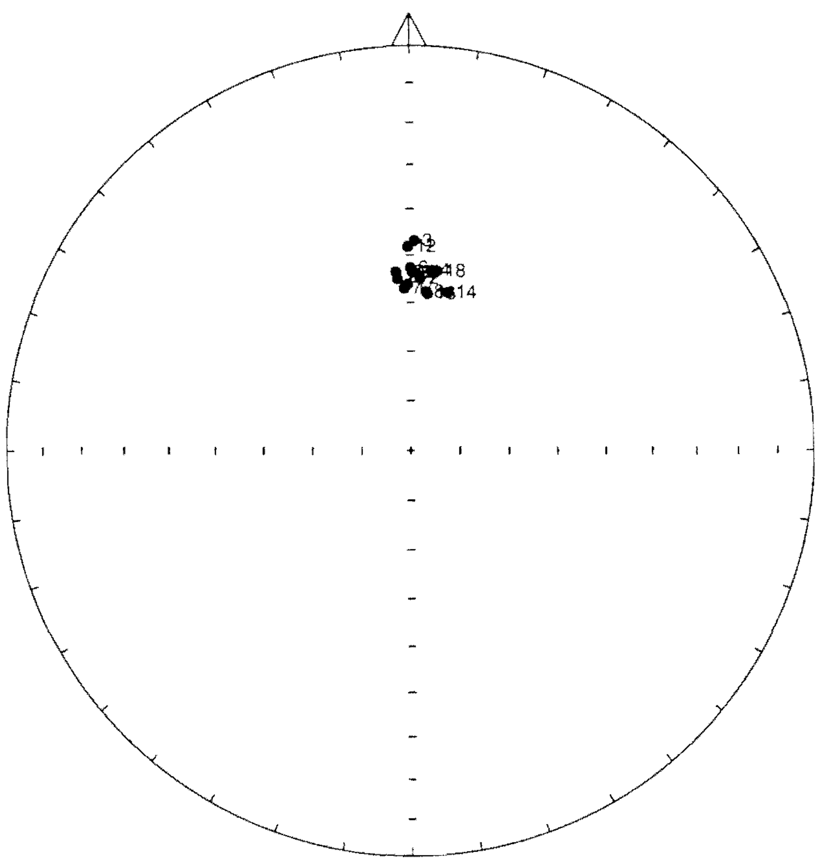

Figure 3: a) Distribution of NRM directions of samples from feature HF represented as an equal area stereogram. In this projection declination increases clockwise with zero being at 12 o'clock while inclination increases from zero at the equator to 90 degrees in the centre of the projection. Open circles represent negative inclinations. b) Distribution of thermoremanent directions of magnetisation of the same samples after partial AF demagnetisation to 5mT.

a)

b)

c)

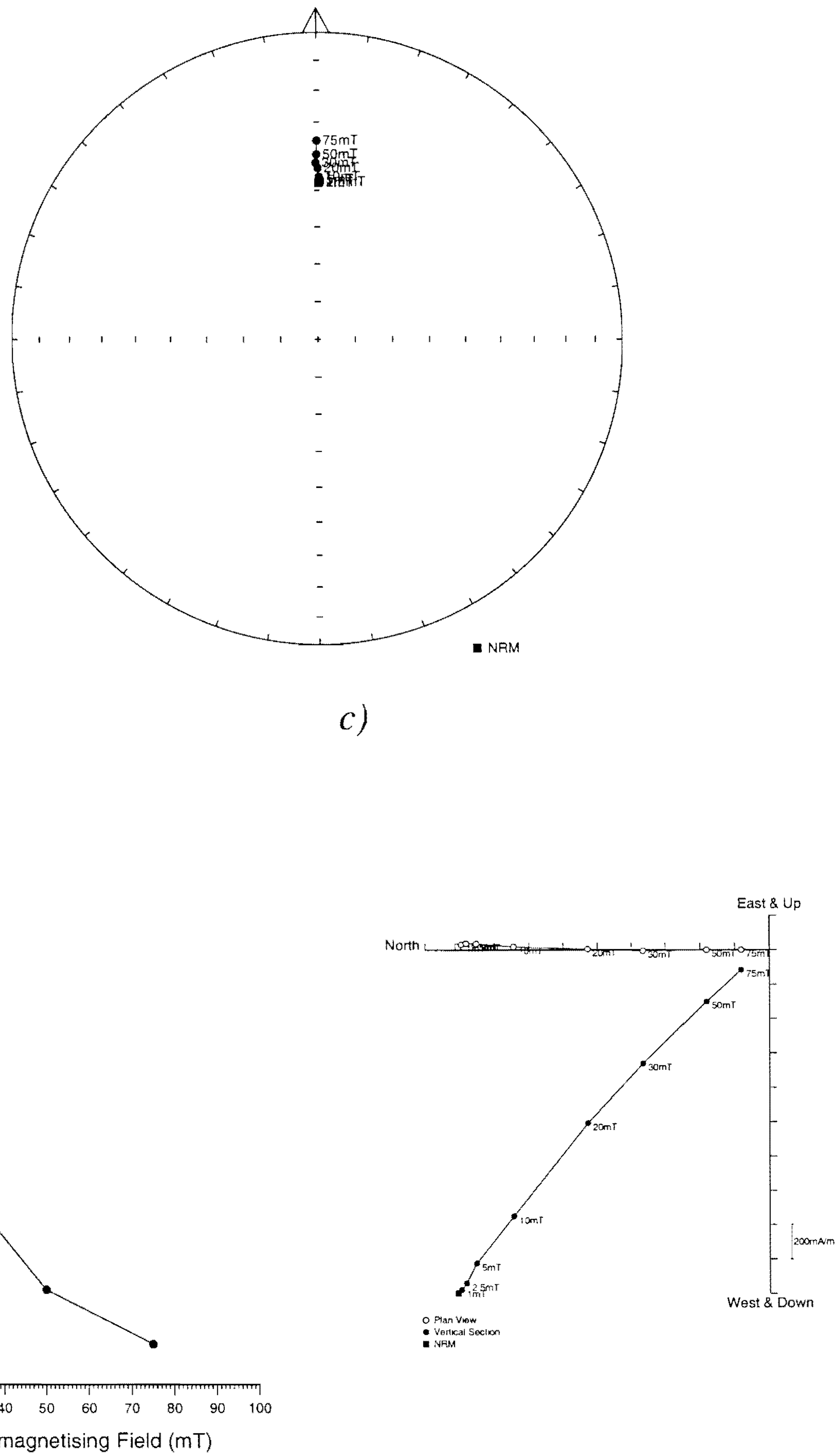

Figure 4: Stepwise AF demagnetisation of sample HF03. Diagram a) depicts the variation of the remanent direction as an equal area stereogram (declination increases clockwise, while inclination increases from zero at the equator to 90 degrees at the centre of the projection); b) shows the normalised change in remanence intensity as a function of the demagnetising field; c) shows the changes in both direction and intensity as a vector endpoint projection.

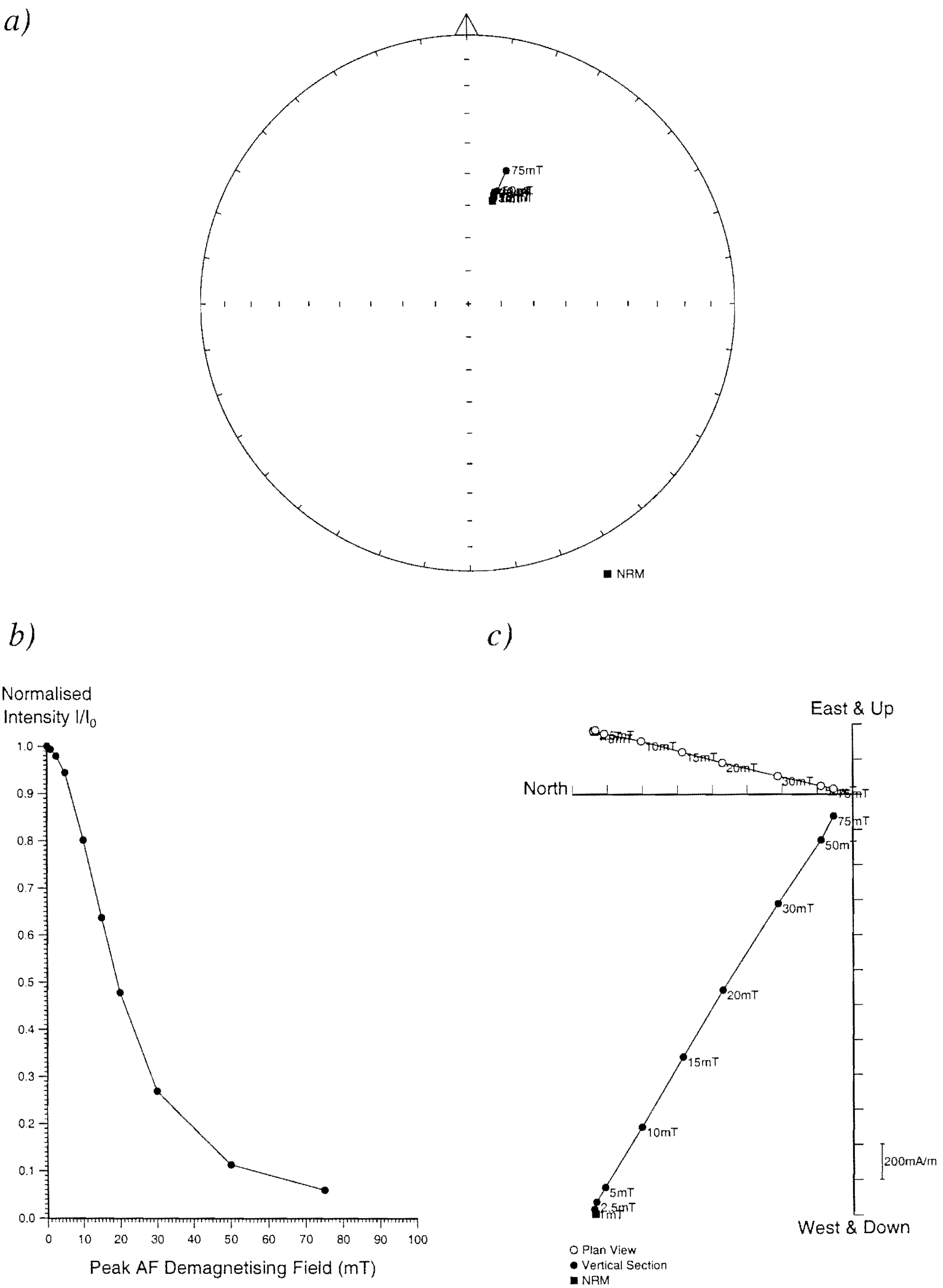

Figure 5: Stepwise AF demagnetisation of sample HF14. Diagram a) depicts the variation of the remanent direction as an equal area stereogram (declination increases clockwise, while inclination increases from zero at the equator to 90 degrees at the centre of the projection); b) shows the normalised change in remanence intensity as a function of the demagnetising field; c) shows the changes in both direction and intensity as a vector endpoint projection.

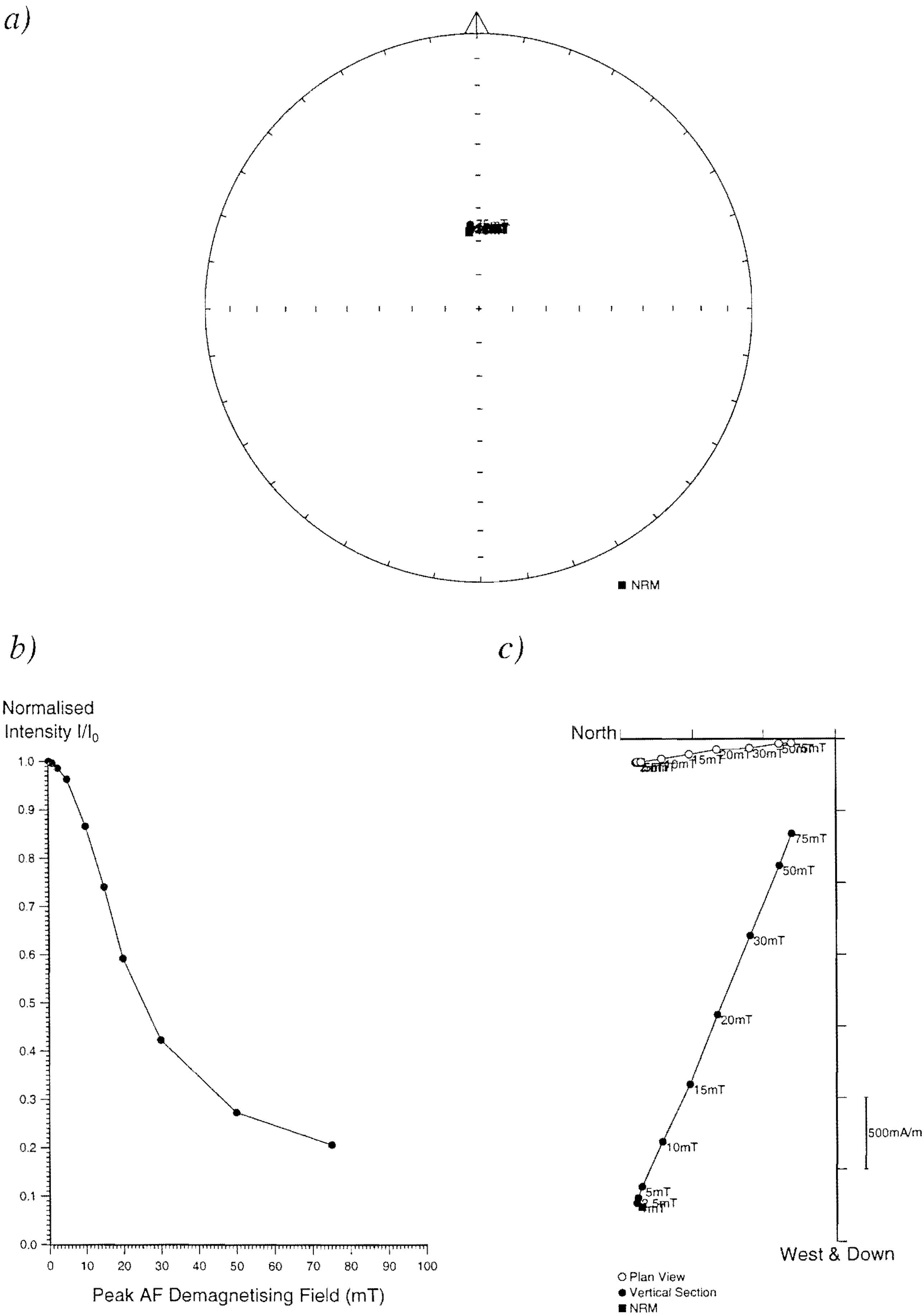

Figure 6: Stepwise AF demagnetisation of sample HF25. Diagram a) depicts the variation of the remanent direction as an equal area stereogram (declination increases clockwise, while inclination increases from zero at the equator to 90 degrees at the centre of the projection); b) shows the normalised change in remanence intensity as a function of the demagnetising field; c) shows the changes in both direction and intensity as a vector endpoint projection.

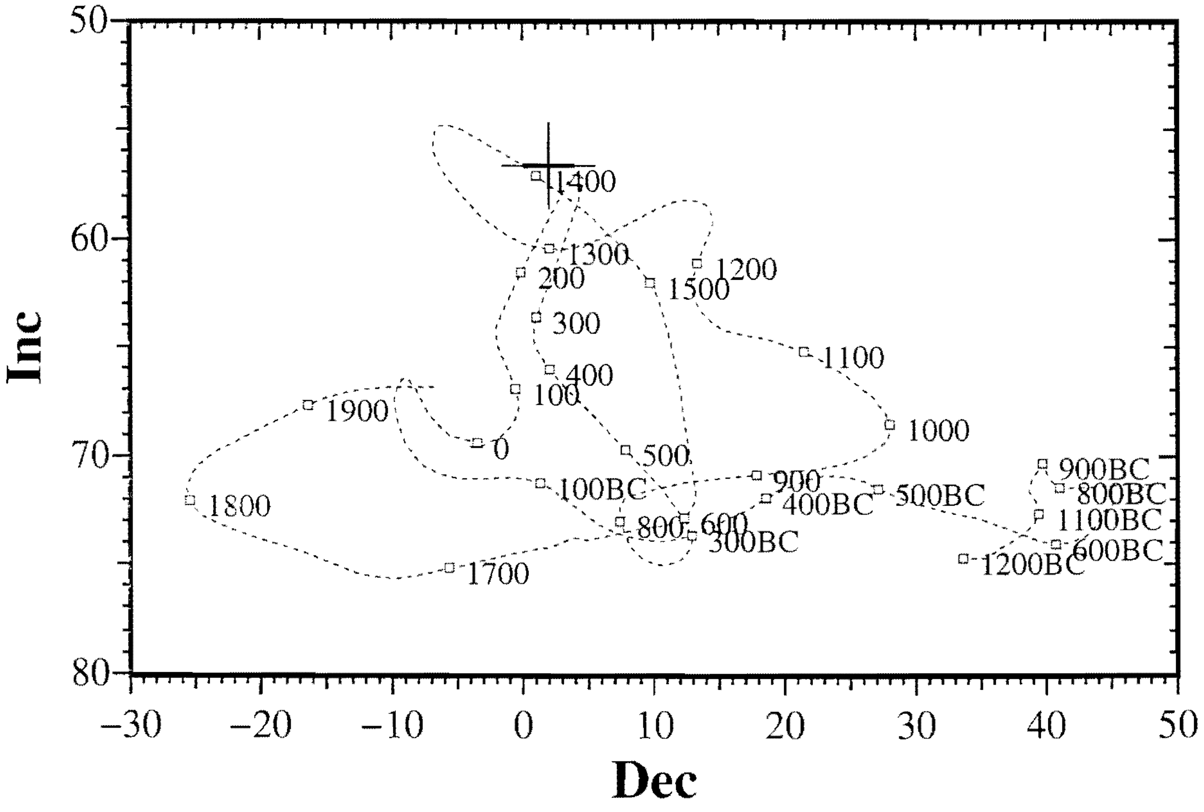

Figure 7: Comparison of the mean thermoremanent vector calculated from samples 02-08, 10-14 and 16-18 from feature HF after 5mT partial demagnetisation with the UK master calibration curve. Thick error bar lines represent 63% confidence limits and narrow lines 95% confidence limits.